ICRF heating in JET during initial operations with the ITER-like wall

P. Jacquet, V. Bobkov, S. Brezinsek, M. Brix, A-L. Campergue, L. Colas, A. Czarnecka, P. Drewelow, M. Graham, C. C. Klepper, E. Lerche, M.-L. Mayoral, A. Meigs, D. Milanesio, I. Monakhov, J. Mlynar, T. Pütterich, A. Sirinelli, D. Van-Eester, and JET-EFDA contributors

ICRF heating in JET during initial operations with the ITER-like wall

P. Jacquet, V. Bobkov, S. Brezinsek, M. Brix, A-L. Campergue, L. Colas, A. Czarnecka, P. Drewelow, M. Graham, C. C. Klepper, E. Lerche, M.-L. Mayoral, A. Meigs, D. Milanesio, I. Monakhov, J. Mlynar, T. Pütterich, A. Sirinelli, D. Van-Eester, and JET-EFDA contributors

Citation: AIP Conference Proceedings **1580**, 65 (2014); doi: 10.1063/1.4864503
View online: http://dx.doi.org/10.1063/1.4864503
View Table of Contents: http://scitation.aip.org/content/aip/proceeding/aipcp/1580?ver=pdfcov
Published by the AIP Publishing

ICRF Heating in JET During Initial Operations with the ITER-Like Wall

P. Jacquet,[a] V. Bobkov,[b] S. Brezinsek,[c] M. Brix,[a] A-L. Campergue,[d] L. Colas,[e] A. Czarnecka,[f] P. Drewelow,[b] M. Graham,[a] C.C. Klepper,[g] E. Lerche,[h] M.-L. Mayoral,[a] A. Meigs,[a] D. Milanesio,[i] I. Monakhov,[a] J. Mlynar,[j] T. Pütterich,[b] A. Sirinelli,[a] D. Van-Eester,[h] and JET-EFDA contributors[*]

JET-EFDA, Culham Science Centre, OX14 3DB, Abingdon, UK
[a]Euratom/CCFE Fusion Association, Culham Science Centre, Abingdon, OX14 3DB, UK.
[b]Max-Planck-Institut für Plasmaphysik, EURATOM-Assoziation, Garching, Germany.
[c]IEK-4, Forschungszentrum Jülich, Association EURATOM-FZJ, Germany.
[d]Ecole Nationale des Ponts et Chaussées, F77455 Marne-la-Vallée, France
[e]CEA, IRFM, F-13108 Saint-Paul-Lez-Durance, France.
[f]Association Euratom-IPPLM, Hery 23, 01-497 Warsaw, Poland.
[g]Oak Ridge National Laboratory, Oak Ridge, TN 37831-6169, USA.
[h]Association EURATOM-Belgian State, ERM-KMS, Brussels, Belgium.
[i]Politecnico di Torino, Department of Electronics, Torino, Italy.
[j]Association EURATOM-IPP.CR, Za Slovankou 3, 182 21 Praha 8, Czech Republic.

Abstract. In 2011/12, JET started operation with its new ITER-Like Wall (ILW) made of a tungsten (W) divertor and a beryllium (Be) main chamber wall. The impact of the new wall material on the JET Ion Cyclotron Resonance Frequency (ICRF) operation was assessed and also the properties of JET plasmas heated with ICRF were studied. No substantial change of the antenna coupling resistance was observed with the ILW as compared with the carbon wall. Heat-fluxes on the protecting limiters close the antennas quantified using Infra-Red (IR) thermography (maximum 4.5 MW/m^2 in current drive phasing) are within the wall power load handling capabilities. A simple RF sheath rectification model using the antenna near-fields calculated with the TOPICA code can well reproduce the heat-flux pattern around the antennas. ICRF heating results in larger tungsten and nickel (Ni) contents in the plasma and in a larger core radiation when compared to Neutral Beam Injection (NBI) heating. Some experimental facts indicate that main-chamber W components could be an important impurity source: the divertor W influx deduced from spectroscopy is comparable when using RF or NBI at same power and comparable divertor conditions; the W content is also increased in ICRF-heated limiter plasmas; and Be evaporation in the main chamber results in a strong and long lasting reduction of the impurity level. The ICRF specific high-Z impurity content decreased when operating at higher plasma density and when increasing the hydrogen concentration from 5% to 20%. Despite the higher plasma bulk radiation, ICRF exhibited overall good plasma heating efficiency; The ICRF power can be deposited at plasma centre and the radiation is mainly from the outer part of the plasma. Application of ICRF heating in H-mode plasmas started, and the beneficial effect of ICRF central electron heating to prevent W accumulation in the plasma core could be observed.

Keywords: Tokamak, JET, ICRF.
PACS: 52.55.Fa, 52.50.Qt

[*] See the Appendix of F. Romanelli et al., Proceedings of the 24th IAEA Fusion Energy Conference, 2012, San Diego, USA.

Radiofrequency Power in Plasmas
AIP Conf. Proc. 1580, 65-72 (2014); doi: 10.1063/1.4864503

INTRODUCTION

In 2011/12, JET started operation with its new ITER-Like Wall (ILW) [1] made of a tungsten (W) divertor and a beryllium (Be) main chamber wall with some recessed W-coated components (e.g. NBI shine-through protection tiles, re-ionisation tiles, restraint ring protections). ICRF heating using the A2 antennas was routinely used to provide central electron heating in support of the experimental program which focused on the characterization of fuel retention with the ILW, characterization of H-mode access and high performance scenario development [2]. Plasma compatibility and performance of ICRF heating (hydrogen minority, deuterium plasma) with the full metallic environment was studied [3]; 5 MW of RF power were launched into L-mode plasmas and up to 4 MW in ELMy H-mode. The main objective of the ICRF experiments in JET with the ILW (JET-ILW) was to verify compatibility of the operation with the ILW environment: (a) Verify if the new wall induced a change in the antenna coupling resistance. (b) Characterize ICRF specific heat loads on PFCs in the vicinity of the antennas. (c) Verify if the use of ICRF with the ILW led to an increased level of W impurity in the plasma. (d) Characterize JET plasmas with ICRF heating, from the point of view of heating efficiency and the effect of central heating on high Z impurity transport.

The JET ICRF heating system includes four "A2" ICRF antennas (A, B, C, and D, see Figure 2). The ITER-Like ICRF antenna (ILA), was not used in 2011/12. Each antenna [4][5] is a phased array of 4 poloidal straps; controlling the phase between straps allows waves to be launched with different $k_{//}$ spectra. Usually π (dipole phasing) or +/- $\pi/2$ phasing (current drive phasings) between adjacent straps are used. The plasma facing part of the antennas is covered by a Faraday screen consisting of tilted solid Be rods. Each antenna is surrounded by two poloidal limiters made of solid Be tiles, and a vertical septum made of solid Be is fitted at the centre of each antenna. During this campaign, antenna C and D were either fed independently or through an External Conjugate-T arrangement with ELM resilience properties [6]; straps 1&2 of antennas A and B were fed by the same RF amplifiers through a 3dB hybrid coupler system [5] also providing ELM resilience. Straps 3&4 of antenna A were fed by independent amplifiers; straps 3&4 of antenna B were not available, consequently only straps 1,2 of antenna A and B could be used on ELMy H-mode plasmas. A numerical model of the A2 antennas has recently been built to be used with the antenna electromagnetic modeling code TOPICA [7] (see Figure 1). TOPICA simulations are now being used to analyze the operation of JET A2 antennas.

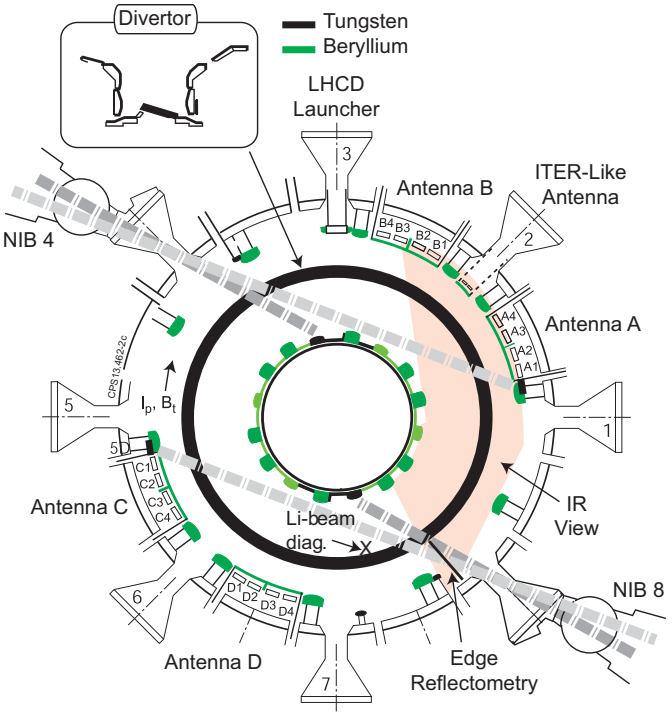

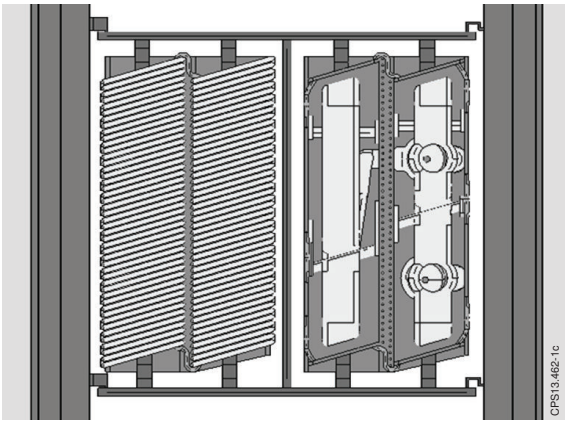

FIGURE 1. Representation of the JET A2 Antenna TOPICA model. The screen bars were removed from the model representation on the right to see straps 1&2.

FIGURE 2. (left) Top view of JET, showing the JET ICRF antennas (A, B, C, D). The IR camera view is in grey. Elements with tungsten surfaces are in black.

A2 ANTENNA OPERATION and RF/SOL INTERACTION

***Antenna Coupling Analysis*:** Given V_{max}, the maximum operating RF voltage in the antenna structure (or in the ICRF system transmission lines) limited by voltage stand-off, the achievable coupled power varies to a first approximation linearly with the antenna coupling resistance R_c: $P_{coupled} \sim V_{\max}^2 \, R_c / 2 Z_c^2$, where Z_c is the transmission line characteristic impedance. The antenna coupling resistance *Rc*, is expected to decrease exponentially with the antenna-fast wave cut-off layer distance [8]. A statistical analysis of *Rc* showed that A2 antennas have similar coupling resistance in JET-ILW, for equivalent midplane outer gap and plasma shape, as in JET with the carbon wall (JET-C). Hence the change in the wall properties, and potentially in the SOL density, has not affected the antenna coupling resistance.

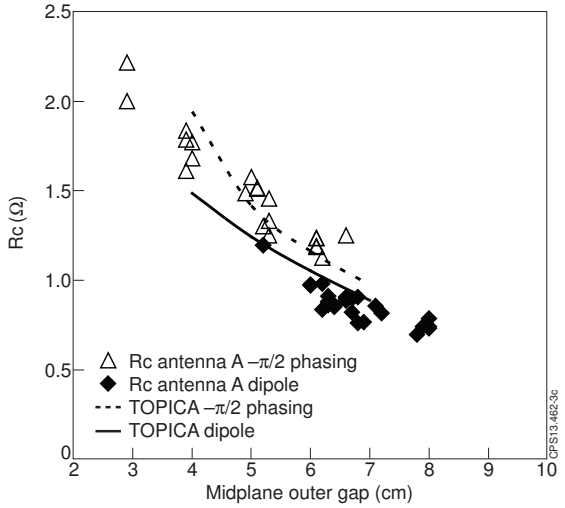

FIGURE 3. Antenna A coupling resistance measured in JET-ILW and results from TOPICA simulations. Only straps 1&2 are powered. The data set includes pulses with line integrated density in the range [$4.5.10^{19}$-$5.5.10^{19}$] m^{-2}.

Preliminary results for the analysis of the A2 antennas *Rc* measurements using TOPICA, are presented in Figure 3**.** For a series of L-mode pulses where the plasma mid-plane outer gap was changed, *Rc* from antenna A is compared to the calculations from TOPICA; in these cases only straps 1&2 were used. The plasma temperature and density profiles representative of the profiles in the L-mode discharges have been used in TOPICA simulations. For dipole phasing, the simulations reproduce well the measured coupling resistance dependence with antenna-plasma distance. For -π/2 phasing, the measured coupling resistance is higher as compared to dipole, this is also reproduced in TOPICA simulations. Further analysis is ongoing to study cases with the 4 antenna straps powered.

***ICRF specific Heat Loads on Antenna Limiters*:** When using ICRF heating, enhanced heat-fluxes are commonly observed on some plasma facing components close to the antennas [9]. Experiments have recently been carried out on JET-ILW to characterize the heat flux to the A2 antennas [10]. Using IR thermography and thermal models of the tiles, heat-fluxes were evaluated from the surface temperature increase during the RF phase of L-mode

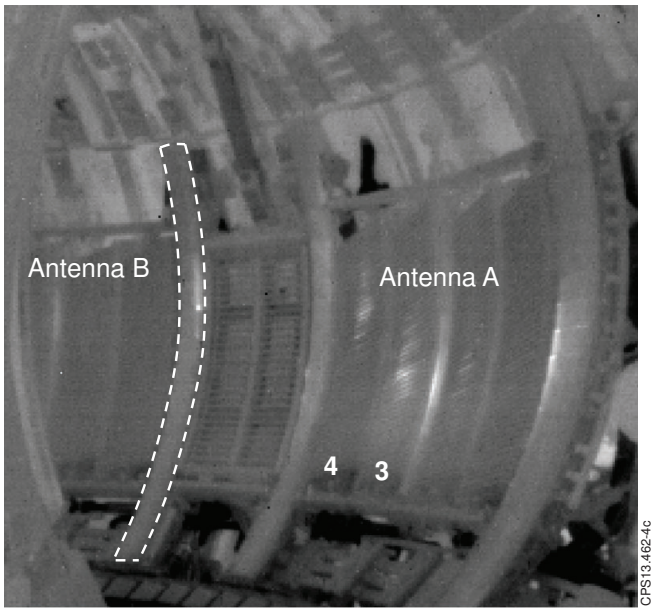

FIGURE 4. Pulse 83063 t=13.0s, IR camera frame showing ICRF hot spots when antenna A (straps 3,4) is powered. The heat-flux on the limiter highlighted with dotted lines is analyzed in Figure 5.

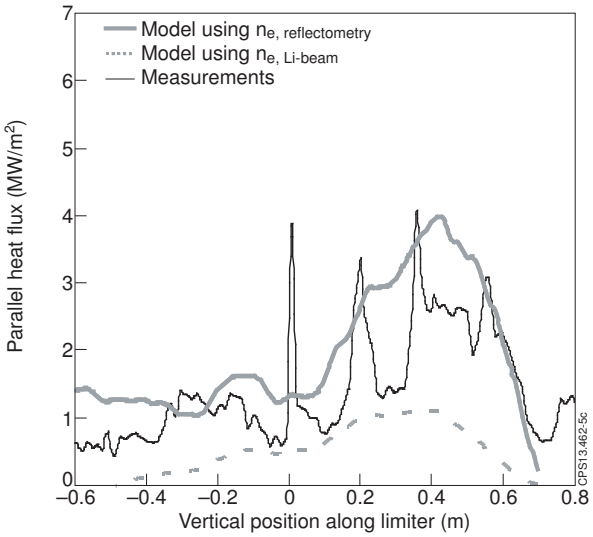

FIGURE 5. Pulse 83603, t=13s, comparison between the heat-flux measured along the poloidal limiter and results from the simple model.

plasmas. The maximum observed heat-flux intensity was ~ 4.5 MW/m^2 when operating with -π/2 strap phasing at power level of 2MW per antenna and with a 4 cm midplane outer gap. The heat-fluxes were enhanced when using current drive phasing and the intensity was found to increase linearly with the density right in front of the antennas and with the square of the RF voltage at the antinodes of the transmission lines feeding the antenna. The Be tiles of the A2s protecting limiters can handle fluxes of the order of 6 MW/m^2 for 10sec, therefore RF specific heat-fluxes are not in practice a limitation for JET ICRF operation (although hot spots need to be monitored). However, these heat-flux values deserve further attention, in particular when compared to the engineering design targets (5 MW/m^2) for the ITER ICRF antenna Faraday screen and neighboring blanket modules.

To optimize the design of the antennas for future devices, modeling activities of ICRF sheath rectification are carried out within the ICRF community (see for example [11]). We have tested a simple RF sheath rectification model in particular to verify if the intensity and the location of the hot-spots measured on the JET antenna protecting limiters is consistent with the $E_{//}$ map in front of the A2s as calculated using the TOPICA code ($E_{//}$ is the RF electric field that drive RF sheath rectification, // denotes the direction parallel to static magnetic field) [12]. In the simplified model derived from [13], $Q_{//} = e Z n c_s V_{DC}$ where *e* is the elementary charge, Z is the atomic number of plasma ions (D_+), c_s is the ion sound speed in the SOL, *n* is the electron density at the antenna and $V_{DC} = \frac{1}{\pi}\left|\int E_{//} dl\right|$ is the RF rectified sheath potential. In the model, the reflectometer or lithium-beam density measurements are mapped along the poloidal limiters to estimate the local density. The $E_{//}$ in front of the antenna is from TOPICA modeling, the field intensity is scaled to the launched ICRF power. The integration to calculate V_{DC} is along the tilted field lines up until the location of the poloidal limiter. A typical result is shown in Figure 5 for pulse 83063 where only strap 3&4 of antenna A were used with -π/2 phasing. The heat-flux estimated from IR thermography along the 2D poloidal limiter is plotted as a function of the vertical height, and it is compared to the estimates from the simple model; the model can reproduce the vertical location of the maximum heat-flux and the magnitude of the heat-flux within the uncertainty of the density measurements. It is important to take into account the variation of *n* along the height of the limiter (plasma-limiter distance is not uniform along the limiter, *n* peaks at ~ 0.3 m) in order for the model to reproduce the location of the maximum load. The model is also consistent with the observed reduced intensity of the hot-spot when the strap phasing is dipole instead of current drive. However the simple model cannot explain the observed experimental scaling of the ICRF specific heat-loads with V^2, more complex phenomena such as the modification of plasma properties in front of the antennas by ICRF power can also be involved explaining this scaling [14].

***ICRF specific impurity source*:** During ICRF heating, the bulk radiated power was found to increase compared to C-wall operation although not preventing efficient heating of the plasma. The radiated power was noticeably higher when using ICRF instead of NBI heating (see Figure 6). The main radiators in the plasma bulk were W (new to the JET-ILW) and Ni (which was also observed in JET-C [15]). The plasma Be content is also higher with ICRF heating. Ni was detected using VUV spectroscopy [15]; W was detected from VUV spectroscopy [16][24]. The analysis of Soft-X Ray (SXR) emission was also used to evaluate the W concentration ($c_{\_W}$) profiles [16]. One could invoke a change in transport of W and Ni in the plasma during ICRF to explain the enhanced level of impurity when using ICRF, but preliminary transport analysis [17] suggest instead that there are specific ICRF Ni and W sources. It was plausible to suspect that RF sheath

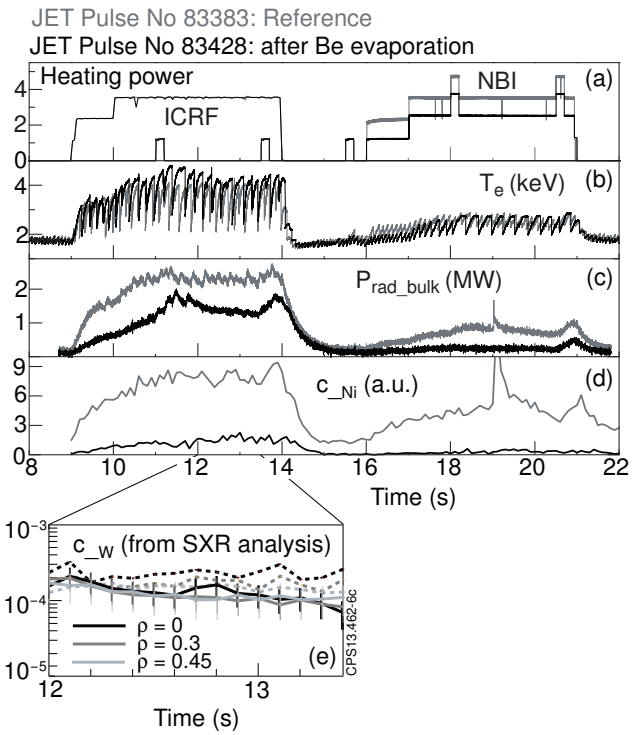

FIGURE 6. For pulse 83383 (before Be evaporation, in grey) and 83428 (after evaporation, in black) time trace of (a) ICRF and NBI power, (b) Te at plasma centre, (c) core radiated power from bolometry and (d) $c_{\_Ni}$ evaluated fromVUV spectroscopy. In (e), $c_{\_W}$ evaluated from SXR analysis at different normalized radius is shown (83383 with dashed lines)

rectification along the field lines which connect the powered antennas to the divertor, could enhance W sputtering in the divertor region. ICRF field – SOL interaction could indeed be evidenced [18]; For example, enhanced Be sputtering was observed using Be I or Be II line spectroscopy with line of sight falling on a limiter close to antenna D or on the Faraday Screen in front of strap 4 of antenna D [19]. The effect was enhanced when using -π/2 strap phasing. Also, the W I emission at the outer divertor baffles, measured with an intensified CCD camera fitted with a 1nm filter (centered at 400.9 nm), was found to change depending on which specific antenna was powered, the effect in this case also enhanced when using -π/2 phasing which is expected to generate higher V_{DC} that drives RF sheath rectification. However we could not directly link the increased W content in the plasma to a specific W source when using ICRF heating. In particular, W line emission spectroscopy [20] did not evidence higher W sputtering in the divertor region when using ICRF heating [18]. The W components located in the main chamber could also contribute importantly to the W in the plasma. In limiter configuration, ICRF heated plasmas also had higher c_W compared to NBI. Moreover, when in such a limiter discharge the plasma was shifted upwards away from the divertor, providing better magnetic isolation between the divertor and the antennas, c_W did not decrease. Further we have investigated the effect of covering the wall with a thin layer of Be through an overnight evaporation (Figure 6). Comparison of reference pulses before/after evaporation (~3 nm thick Be layer) shows a strong reduction of the Ni and W concentration level, and of the bulk radiated power. The effect was still visible after ~10 ELMy H-modes pulses. This is consistent with the idea that Ni and W remote areas in the main chambers were screened from sputtering by the Be layer which suggests that these areas contribute significantly to the high Z impurity source in JET. The possible mechanisms responsible for enhanced sputtering of W and Ni during RF are: (a) near field RF sheath rectification; (b) far field RF sheath rectification; (c) charge exchanged neutrals of RF accelerated fast particles.

ICRF PLASMA HEATING

Plasma parameters and high Z impurity content: The edge density is a key parameter that influences the plasma impurity content, c_W [18] and c_{Ni} [24] being both reduced when operating at higher density. A number of different processes could lead to this result: a) a decrease of the impurity source from a reduced electron temperature in the SOL when operation at higher density (using higher level of gas dosing); b) a change in impurity transport properties; c) a direct dilution of the impurities in the plasma.

An experiment was run to investigate the effect of the hydrogen minority concentration on impurity concentration; working at H concentration of ~ 15% - somewhat higher than the few percents traditionally used for minority heating - reduced the W and Ni concentration and the bulk radiation. Impurity concentration and radiated power increased again when further increasing the H fraction above 20 %. A tentative explanation for these observations has been proposed in [25]: Increasing the hydrogen fraction on one hand increased the edge density, which enhanced the antennas coupling resistance and reduced the antenna electric field thus reducing RF sheath rectification effects. But it also reduced the absorption efficiency which increased the power fraction re-incident on

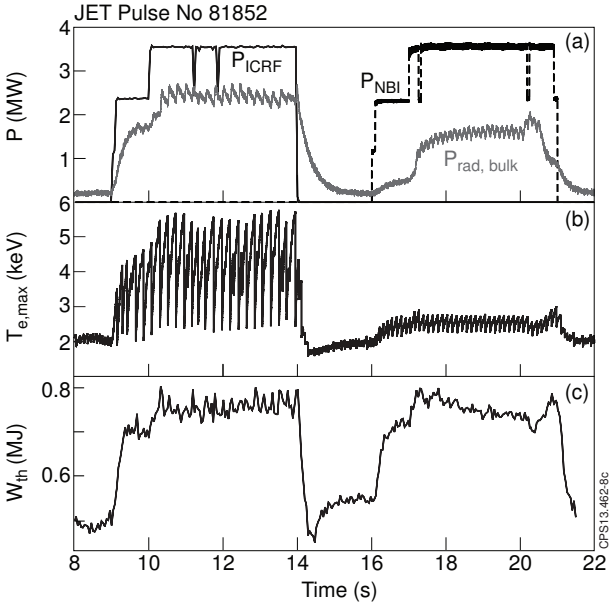

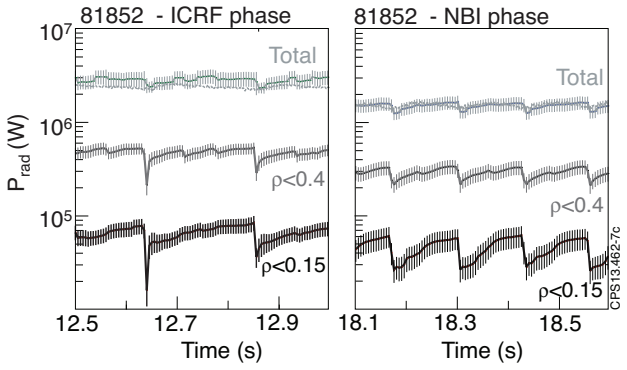

FIGURE 7. Radiated power (from bolometry and SXR analysis) during the ICRF and NBI phase for pulse 81852; total from plasma bulk (light grey), radiated inside normalized radius (ρ) of 0.4 (grey) and inside ρ=0.15 (black).

FIGURE 8. (Left) For pulse 81852, (a) time trace of ICRF and NBI power and power radiated in core plasma (grey line); (b) central electron temperature; (c) Thermal energy.

the edge, the latter hindering coupling. We should also add that for the pulses with low H concentration, the plasma entered into M-mode (regime with enhanced particle confinement [26]); this change in confinement regime could be involved in the observed changes in the SOL density when varying the H fraction. The effect of the M-mode of the high Z impurity transport at the edge barrier could also not be ruled-out.

***ICRF heating efficiency*:** During the initial campaign of JET_ILW, H minority heating in D was almost exclusively used, with the cyclotron resonance either on-axis or off-axis. Except for specific experiments reported in the previous paragraph H_2 was injected to establish a H fraction of ~5%. This heating regime, leads mainly to power deposition on the bulk electrons by collisions with the ICRF - accelerated H ions, and it generally has good single pass wave absorption. The heating efficiency was found similar than for JET-C. The plasma heating capabilities of NBI and ICRF waves were also found similar [21]. The heating performance of ICRF waves is further illustrated in Figure 7 and Figure 8 from [23]. Pulse 81852 is a L-mode plasma (Bt=2.55T, Ip=2MA, $n_{e,0}=2.4\times10^{19}m^{-3}$) with a ICRF phase (f=42 MHz) and a NBI phase (3.5 MW input power in both cases); despite the larger W and Ni impurity content during RF (see [23]) and the larger radiated power in the plasma bulk (1.5 larger), the plasma thermal energy is similar for both phases. Two important factors contribute in preserving the overall ICRF heating efficiency. First, ICRF waves heat efficiently the electrons in the plasma centre as shown from the central electron temperature increase (Figure 8-b). Second, plasma radiates power mainly from the outer part as is shown in Figure 7 from bolometric signals and SXR signals analysis. During the RF phase, less than 20% of the total radiated power comes from $\rho<0.4$ and less than 3% from $\rho<0.15$.

Use of ICRF heating in H-mode plasmas: H-mode plasmas with the JET-ILW are prone to W accumulation if reducing the gas dosing too much [2]; indeed, a higher level of gas injection contributes to increase the ELM frequency and reduce the intensity of impurities source. But it also affects the plasma energy confinement [27]. Central electron heating was proved efficient on ASDEX Upgrade to increase local transport of high Z impurities and prevent accumulation [28]. Although ICRF heating was used in the H-mode plasmas only late in the campaign, we have indications that this tool can be used in JET-ILW to prevent impurity accumulation. This is pictured in figures 9, 10, 11 and 12 for pulse 83897 (Bt=2.65 T, Ip=2MA, 15.9 MW NBI) and pulse 83603 (same plasma, 14.5 MW NBI and 3.5 MW ICRF heating). Due to the slightly lower NBI power in 83603, the ELM are less frequent before the ICRF phase and impurity flushing by the ELMs at the edge transport barrier is less efficient, hence the increased total radiated power for 83603 at the beginning of the H-mode phase. The central electron temperature (figure 11-b and 12-b) is higher in pulse 83603 when using central ICRF heating; in both pulses infrequent sawteeth are present (~350 ms period in 83597 and ~400 ms in 83603). In 83597 the central temperature is decreasing halfway through the sawteeth period, before the crashes, indicating radiating cooling in the plasma centre. This is confirmed by the radiation emission peaked at the centre as measured by bolometry (not shown) and SXRs (Figure 10-a). Tungsten concentration in these plasmas was evaluated from the anaylsis of SXR emission [29]. The result is shown in Figure 11-a and 12-a. For the no-RF case, c_W peaks at the centre up to values in the order of 10^{-3}. With ICRF heating in 83603 c_W at mid radius is larger than for NBI heating only, consistent with the overall larger plasma radiation (Figure 9-c), but tungsten peaking in the center is much less pronounced, c_W at the centre even decreases in the second half of the sawtooth cycles. This result illustrates the potential of central ICRF heating to prevent W accumulation in JET-ILW plasmas.

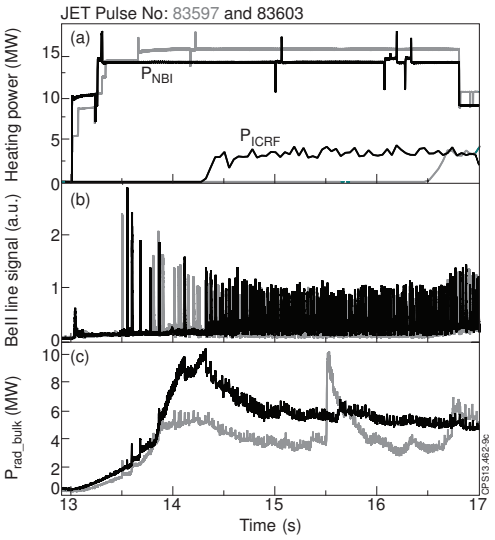

FIGURE 9. For pulse 83603 (black) and 83597 (grey) traces of (a) heating power, (b) Be II line emission (ELMs) and (c) bulk radiated power.

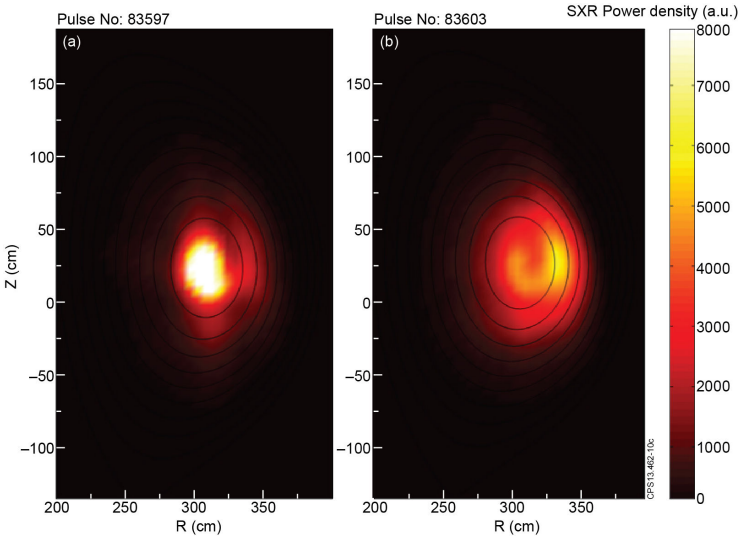

FIGURE 10. tomographic reconstruction of SXR emission right before a sawtooth crash: (a) 83597 t=15.3151s, and (b) 83603 t=15.3451s. SXR data are averaged over 10 ms.

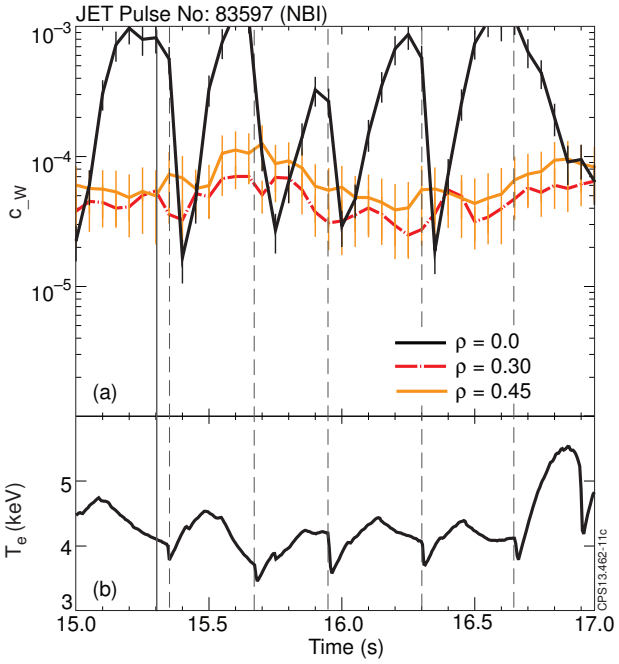

FIGURE 11. For pulse 83597 with no ICRF, (a) c_W estimated from SXR emission profile at normalized radius ρ=0.0, ρ=0.3 and ρ=0.45 and (b) Te at plasma centre. The vertical solid line indicates time when SXR emission profiles are plotted in Figure 10.

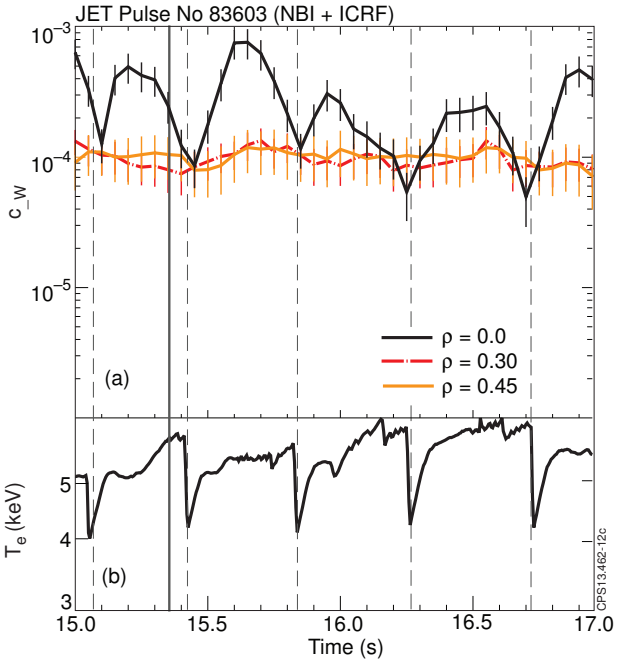

FIGURE 12. Same as **FIGURE 11**, but for pulse 83603 with 3.5 MW of ICRF heating.

CONCLUSIONS

At JET, the ICRF system operation did not encounter limitation from the change from the carbon wall to the ILW. In L-mode, radiation from bulk plasma and impurity levels are higher, but generally the ICRF heating is efficient and plasma does not exhibit peaked centre radiation. In addition, we have indications that ICRF central heating is efficient in H-mode plasmas to prevent W accumulation. In the JET campaign starting in summer 2013

more power will be available in H-mode (straps 3,4 from antenna A and B will be available in the ELM resilient configuration). The emphasis will be on the optimization of the use of ICRF heating to prevent W accumulation, using the ICRF capabilities to provide central electron heating and as a tool for MHD activity control [30].

AKNOWLEDGEMENTS

This work, part-funded by the European Communities under the contracts of Association between EURATOM and CCFE, was carried out within the framework of the European Fusion Development Agreement. The views and opinions expressed herein do not necessarily reflect those of the European Commission. This work was also funded by the RCUK Energy Programme under grant EP/I501045.

REFERENCES

[1] G. F. Matthews*, et al.,* Physica Scripta **T128** (2007) 137–143
[2] R. Neu, *et al.,* Physics of Plasmas **20**, 056111 (2013)
[3] M-L. Mayoral, *et al*., On the challenge of plasma heating with the JET metallic wall, in Proceedings of 24th IAEA Fusion Energy Conference (San Diego, USA, 2012), EX/4-3
[4] A. Kaye, *et al.*, Fusion Engineering and Design **24** (1994) 1-21
[5] M. Graham, *et al*., Plasma Phys. Control. Fusion **54** (2012) 074011 (11pp)
[6] I. Monakhov, *et al*., Nucl. Fusion **53** (2013) 083013 (21pp)
[7] D. Milanesio, *et al*., Nucl. Fusion **49** 115019 (2009)
[8] Bilato R., Brambilla M., Hartmann D.A. and Parisot A. 2005 Nucl. Fusion **45** L5–7
[9] P. Jacquet, *et al.,* Nucl. Fusion **51** (2011) 103018 (16pp)
[10] P. Jacquet, *et al.*, Journal of Nuclear Materials **438** (2013) S379–S383
[11] J. Jacquot, *et al*., Radio-frequency Sheath Physics / Experimental Characterization on Tore Supra and Related Self-consistent Modeling, these proceedings
[12] A.-L Campergue, *et al*., Characterization of local heat flux around ICRF antennas on JET, these proceedings
[13] L. Colas*, et al*., Journal of Nuclear Materials **390–391** (2009) 959–962
[14] M. Becoulet, *et al.,* 2002 Phys. Plasmas **9** 2619–32
[15] A. Czarnecka, *et al*. 2012 Plasma Phys. Control. Fusion **54** 074013
[16] T. Pütterich, *et al*.,Tungsten screening and impurity control in JET, in Proceedings of 24th IAEA Fusion Energy Conference (San Diego, USA, 2012), pp. EX/P3–15
[17] D. Kalupin, *et al.*, Submitted to Nuclear Fusion
[18] V. Bobkov, *et al.,* Journal of Nuclear Materials **438** (2013) S160–S165
[19] C. Klepper, *et al.*, Journal of Nuclear Materials **438** (2013) S594–S598
[20] A.G. Meigs, *et al*., Journal of Nuclear Materials **438** (2013) S607–S611
[21] Van Eester D, *et al.*, 2012, Characterization of Ion Cyclotron Resonance Heating in presence of the ITER-like wall in JET Proc. 39th EPS Conference & 16th Int. Congress on Plasma Physics P1.094
[22] E. Lerche, *et al.*, Statistical analysis of the ICRF and NBI heating performances in L-mode, these proceedings
[23] M-L. Mayoral*, et al*., Comparison of ICRF and NBI Heated Plasmas Performances in the JET ITER-Like Wall, these proceedings
[24] A. Czarnecka, *et al.*, Spectroscopic Investigation of Heavy Impurity Behaviour During ICRH with the JET ITER-Like Wall, these proceedings
[25] Van Eester D, *et al.*, Hydrogen minority ion cyclotron resonance heating in presence of the ITER-Like Wall in JET, these proceedings
[26] ER. Solano, *et al*., M-mode: axi-symmetric magnetic oscillation and ELM-less H-mode in JET, 40th EPS conference on Plasma Physics, Espoo, Finland (2013)
[27] G. Saibene, *et al.* 1999 Nucl. Fusion **39** 1133–56
[28] C. Angioni, Phys. Plasmas **14** (2007) 055905.
[29] T. Pütterich, *et al*., Taming Tungsten in JET and ASDEX Upgrade40th EPS conference on Plasma Physics, Espoo, Finland (2013)
[30] J.P. Graves, *et al*., (2012) Nature Communications 3, 624 doi:10.1038/ncomms1622